Marcel Dekker, New York (1978).
29. A. P. Tomilov and N. E. Chomutov, *ibid.,* Vol. III, p. 1 (1975).
30. C. D. Thurmond, *J. Phys. Chem. Solids,* **26,** 785 (1965).
31. M. P. Dare-Edwards, A. Hamnett, and J. B. Good-
enough, *J. Electroanal. Chem. Interfacial Electrochem.,* **119,** 109 (1981).
32. H. Kita and T. Kurisu, *J. Res. Inst. Cat. Hokkaido Univ.,* **21,** 200 (1973).
33. R. H. Wilson, *J. Appl. Phys.,* **48,** 4292 (1977).
34. R. H. Wilson, *This Journal,* **127,** 228 (1980).

Semiconductor Electrodes

XXXVII. Photoelectrochemical Behavior of p-Type Cu_2O in Acetonitrile Solutions

G. Nagasubramanian, Alberto S. Gioda, and Allen J. Bard*

Department of Chemistry, The University of Texas, Austin, Texas 78712

ABSTRACT

The photoelectrochemical behavior of polycrystalline p-Cu_2O in acetonitrile solutions containing a number of redox couples [*e.g.,* phthalonitrile (0/−1), nitrobenzene (0/−1), methyl viologen (+2/+1)] was investigated. The p-Cu_2O, grown by oxidation of Cu metal by thermal methods or anodization, showed stable behavior under optical irradiation in these solutions. The bandgap, estimated from photoacoustic spectroscopy (PAS) and the photocurrent action spectrum in solution, was ~2.0 eV and the flatband potential was ~ +0.16V *vs.* SCE. Scanning electron micrographs of the thermally grown samples reveal well-developed crystallites with distinct boundaries. A PEC cell of the form p-Cu_2O/Ph$(CN)_2$,MeCN/Pt was shown to have an overall optical-to-electrical energy conversion efficiency of only 0.05%. The low efficiency for such a cell is ascribed to rapid recombination processes in the bulk semiconductor and at the interface.

Cuprous oxide (Cu_2O), which crystallizes in a cuprite structure is a catalyst of choice for a diverse variety of chemical reactions (1-4). The optical and electrical properties of p-Cu_2O depend upon the conditions of preparation from Cu and O_2, *i.e.,* the temperature and oxygen pressure (5). Several workers (6-11) have studied the electrical properties of single crystals of this material and demonstrated that it is a p-type semiconductor whose hole conductivity can be attributed to copper ion vacancies which act as acceptors for electrons from the valence band. Recently, Trivich *et al.* (12) studied solid-state photovoltaic cells based on this material and reported an overall conversion efficiency of optical to electrical energy approaching 1% and stated that efficiencies of 6-12% should be possible. Aqueous photoelectrochemical (PEC) cells involving p-Cu_2O have also been described (13-14). In these cells the p-Cu_2O photocathode is unstable and under irradiation is reduced to Cu metal

$$Cu_2O + 2H^+ + 2e \rightarrow 2Cu + H_2O \qquad [1]$$
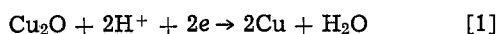
Similar instability was observed with CuO electrodes (15). In an aprotic solvent such as acetonitrile (MeCN), however, such a reduction reaction is less favorable because of the unavailability of protons. Since the bandgap is 1.9-2.0 eV, and the reported efficiencies for photovoltaic devices appeared interesting and the material is inexpensive, abundant, and capable of being readily produced in thin film form, we undertook a study of the PEC properties of p-Cu_2O prepared by thermal and anodic oxidation of metallic copper in MeCN. The polycrystalline compacts were prepared by heating a Cu plate in air to minimize the grain boundary effects encountered in the case of sintered powder compacts (16). Studies of the PEC behavior of p-Cu_2O were carried out with MeCN con-

taining several redox couples including phthalonitrile, Ph$(CN)_2$(0/−1), nitrobenzene, PhNO$_2$(0/−1), and methyl viologen MV (+2/+1). Photocathodes of p-Cu_2O were shown to be stable in these solutions under intense optical irradiation. However, the overall optical-to-electrical energy conversion efficiencies in the PEC cells based on this material were low (< 0.1%).

Experimental

Chemicals.—The procedures for the purification of chemicals and solvent (MeCN) are given elsewhere (17). All compounds were stored inside a helium-filled Vacuum Atmosphere Corporation (Hawthorne, California) glove box. Polarographic grade, tetra-n-butyl ammonium perchlorate (TBAP), dissolved and recrystallized from ethanol thrice and dried under vacuum (< 10^{-5} Torr) for three days, was used as supporting electrolyte. The cell employed was a conventional two-compartment cell of 25 ml capacity containing the p-Cu_2O, a Pt counterelectrode, and a quasi-reference electrode which was an Ag wire immersed in the solution and separated from the main compartment by a medium porosity glass frit. The potential of the electrode was checked against an aqueous saturated calomel electrode (SCE) at regular intervals and was found to be constant. All potentials reported here, unless specified otherwise, are given in V *vs.* SCE.

P-Cu_2O was prepared by the method of Trivich *et al.* (12, 18). A Cu plate, 0.8 mm thick (Alfa Ventron), was cut to a 2 × 2 cm square, polished with Al_2O_3 (0.5 μm), washed with acetone, and rinsed thoroughly with double distilled water. The plates were dried and heated in a muffle furnace at about 900°C for 24 hr. Subsequently, the furnace temperature was raised to 1030°C and the samples were heated for an additional 160 hr. The furnace temperature was then reduced to 500°C and at this temperature, the samples were annealed for a day, before quenching them in air at room temperature. Upon quenching, the CuO layer formed

at the surface peels off, exposing the Cu_2O sintered compacts. The resistivity of the material after polishing with an ultrafine emery paper was $\sim$ 30-40 Ω cm. An ohmic contact can be formed by either electroplating the back with gold or partial reduction in an H_2 atmosphere at 100°-125°C for 30 min. A copper wire lead formed the electrical contact and was attached to the gold-coated side with silver epoxy cement (Allied Product Corporation, New Haven, Connecticut). This contact was subsequently covered with 5 min epoxy cement. The assembly was mounted into 7 mm diam glass tubing and was held in position with a silicone rubber sealant (Dow Corning Corporation, Midland, Michigan), which also served as an effective seal against the seepage of electrolyte solution to the rear of the semiconductor electrode. The exposed area of p-Cu_2O was 0.14 cm². The etching procedures are given below. The material produced by the Cu-air reaction was shown to be Cu_2O by x-ray diffraction. The x-ray diffraction patterns corresponded to those reported in the literature (ASTM card Index No. 5.0667).

The p-Cu_2O films formed by anodic polarization of a Cu electrode were grown under either linear potential sweep or constant current conditions in aqueous NaOH solutions, mainly, following the procedures described by Marchiano et al. (19) and Ashworth and Fairhurst (20). The pretreatment of the Cu electrodes prior to oxidation described in the above papers was employed. Prepurified N_2 was bubbled for 1 hr through the NaOH solutions, prior to and during the experiments, and an N_2 atmosphere was maintained over the solutions during the anodizations. The potential sweeps were performed at scan rates of 0.02, 0.2, or 1.0 mV/sec with the initial potential at −0.8V (for 0.02 mV/sec) or −1.20V (for 0.2 and 1.0 mV/sec) vs. SCE. The galvanostatic runs were performed at the current densities reported in Ref. (20).

Apparatus.—A Princeton Applied Research (PAR) Model 173 potentiostat and PAR Model 175 Universal programmer were used in all experiments with positive feedback iR-compensation employed to compensate for solution resistance and internal resistance of the electrode. The i-V curves were recorded on a Model 2000 X-Y recorder (Houston Instruments, Austin, Texas). In solar cell experiments, the photovoltage and photocurrent between the working electrode and counterelectrode as a function of load resistance were measured with a Keithley Model 179, TRMS Digital Multimeter. The light source was an Oriel Corporation (Stamford, Connecticut) 450W xenon lamp. Differential capacitance was measured with a PAR Model HR 8 lock-in amplifier. All of these solutions were prepared in the glove box and the cell then sealed and removed for the experiments.

Etchants.—(A) For thermally grown p-Cu_2O, the following etchants were tried: (1) 12M HNO_3, (2) 6M HNO_3, (3) H_2SO_4:H_2O_2:H_2O; 3:1:1 (by volume), (4) HNO_3:H_3PO_4:acetic acid; 17:41.5:41.5 (by volume). In etchants (1), (2), and (3), the etching time was limited to 10-15 sec while for (4) the samples were kept immersed for 15 min. Procedure (1) exposed well-developed large Cu_2O-crystallites while (2) and (3) showed small Cu_2O crystallites. Procedure (4) produced a smooth and shiny surface. (B) The anodically produced films were etched with either (1) 0.01M or (2) 0.1M HNO_3 for 1-2 sec.

Results and Discussion

Capacitance measurements.—The location of the energies corresponding to the edges of the valence and the conduction bands, E_v and E_c, respectively, of the semiconductor electrode with respect to solution energy levels, is useful in the selection of appropriate redox couples for optimizing PEC cell performance. These are usually found by determination of the flatband potential, V_{FB}, by measurement of the electrode capaci-

tance as a function of applied potential. If this capacitance corresponds to the semiconductor space-charge capacitance, V_{FB} and the acceptor density (N_A) can be computed from Mott-Schottky plots (21-23). From these values, the known or estimated effective mass of charge carrier and the bandgap, the band positions (i.e., E_c and E_v) can be located.

A dielectric constant of 7.11 (24) and an effective mass of charge carriers $0.84m_o$ (25) was employed. The bandgap was measured by two methods which are described in the next section; the value determined from the photocurrent action spectrum was employed in the location of the bandedge. The capacitance of p-Cu_2O was measured in MeCN containing TBAP as supporting electrolyte at different frequencies from 100 to 5000 Hz; Mott-Schottky plots are given in Fig. 1. The V_{FB} value determined at low frequencies (100 and 500 Hz) was located $\sim$ 20 mV positive of that at high frequencies (2 and 5 kHz). Hence, an average value was taken for computation. These plots were essentially the same after repeated experiments over several hours and were unaffected by the addition of the reducible compound phthalonitrile to the solution. From these plots we estimate V_{FB} as + 0.16V vs. SCE and $N_A \cong 4.9 \times 10^{16}$ cm⁻³.

Bandgap.—The bandgap energy, E_g, of p-Cu_2O was determined by two independent methods: From the photoacoustic spectrum of the sample in air (26) and from the photocurrent action spectrum in MeCN/TBAP, $Ph(CN)_2$. The results of these experiments are shown in Fig. 2(a) and (b). Note that a plot of $(\eta h\nu)^2$ vs. $h\nu$ gives a straight line, suggesting that the optical transition in Cu_2O is direct and yields an E_g of 2.00 eV. The photoacoustic spectrum signals an onset of light absorption at 638 nm, corresponding to an $E_g =$ 1.94 eV. The bandedge energies were obtained by assuming the Fermi-Dirac equation

$$N_A = N_v [1 + 2e^{(E_v - E_t)/kT}]^{-1} \qquad [2]$$

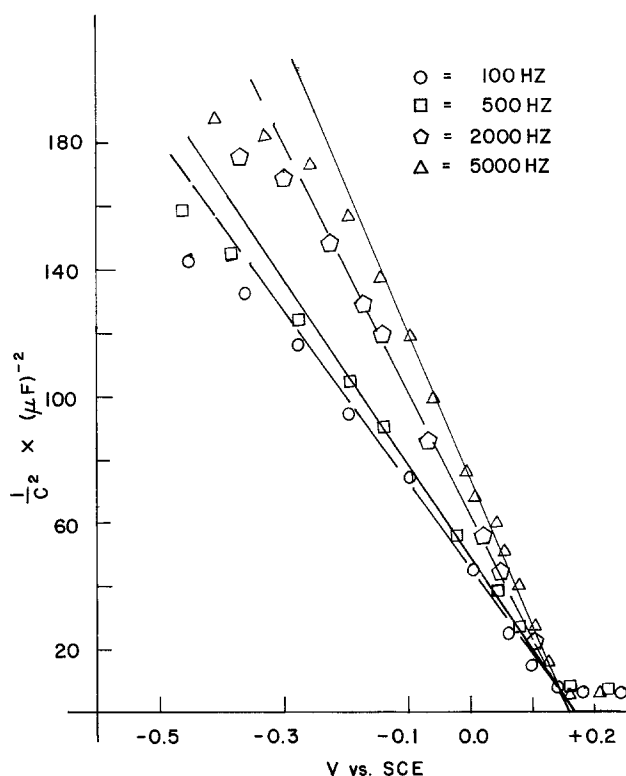$$N_v = 2(2\pi m_p^* kT/h^2)^{3/2} \qquad [3]$$

Fig. 1. Mott-Schottky plot of p-Cu_2O, in MeCN containing 0.1M TBAP supporting electrolyte. $\bigcirc$ = 100 Hz; $\square$ = 500 Hz; $\diamondsuit$ = 2000 Hz; and $\triangle$ = 5000 Hz.
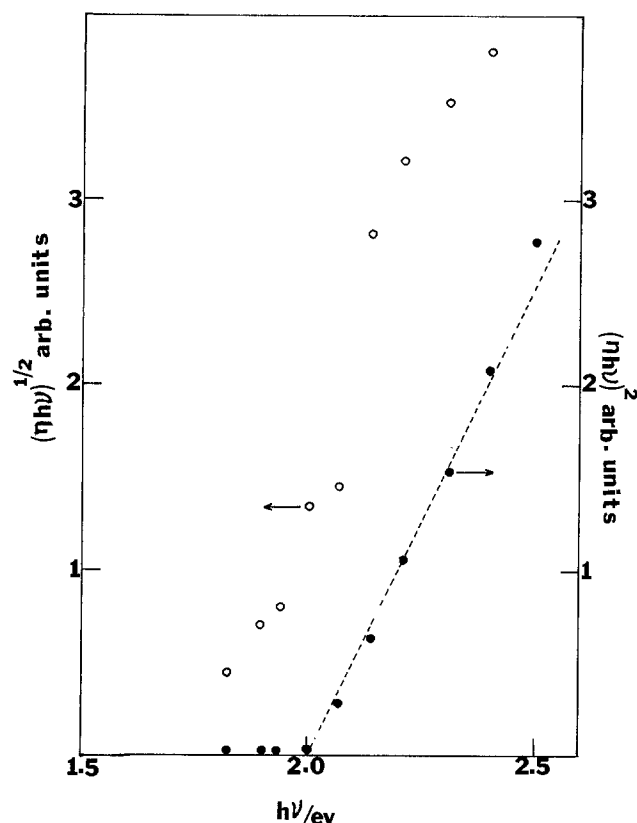
Fig. 2a. Plot of $h\nu$ vs. $(\eta h\nu)^{n/2}$ where $n = 1$ and 4. The value of η at different wavelengths has been computed from photocurrent action spectrum for p-Cu_2O in MeCN/0.1M TBAP, 10 mM Ph(CN)$_2$$^{0/-1}$/Pt solar cell.
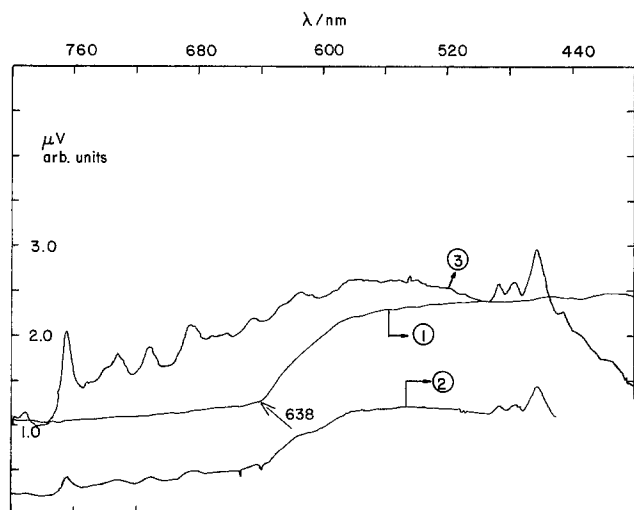

Fig. 2b. Absorption spectrum of p-Cu_2O (photoacoustic technique) (curve 2). Corrected action spectrum of the short-circuit photocurrent of p-Cu_2O (curve 1). Curve 3, background action spectrum of the 2.5 kW xenon lamp.

where N_v is the density of states in the valence band; E_f is the Fermi level energy (corresponding to V_{FB}); and m_p* is the effective mass of holes. This yielded the position of the VB edge about 0.1 eV below the Fermi level, *i.e.*, at $+$ 0.26V *vs.* SCE. From the value of E_g, 2.0 eV, E_c is placed at $-$ 1.74V *vs.* SCE. These levels are shown in Fig. 3, along with the potentials for the solution redox couples employed in this study.

Cyclic voltammetry.—To study the photoinduced electron transfer to reducible molecules in solution, the cyclic voltammetric (CV) response at p-Cu_2O in the dark and under illumination was compared to that ob-

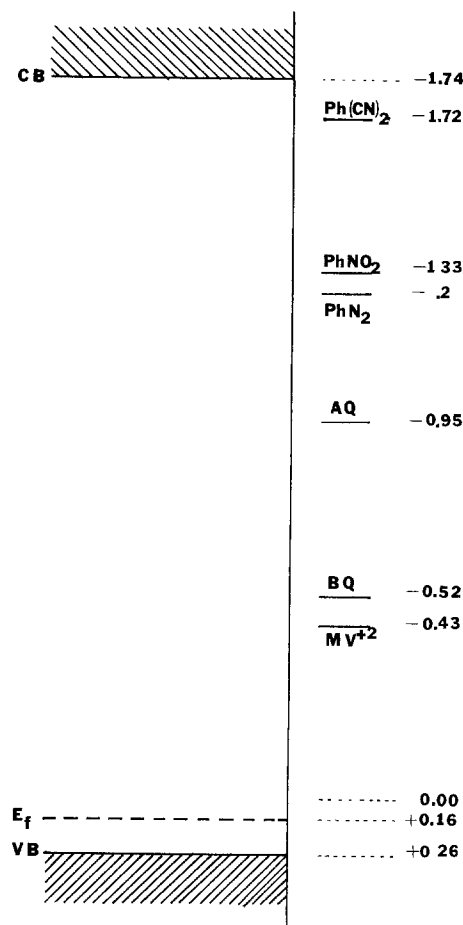**Fig. 3.** Schematic representation of the energetic situation at p-Cu_2O/solution interface along with V_{redox} of various redox couples investigated in this work. CB = conduction bandedge; E_f = Fermi level; VB = valence bandedge; Ph(CN)$_2$ = phthalonitrile; Ph(NO$_2$) = nitrobenzene; AB = azobenzene; AQ = anthraquinone; BQ = benzoquinone; MV^{2+} = methyl viologen dication.

served for these systems at a platinum electrode. At platinum, near-reversible CV behavior is observed, so that the redox potential of the couple can be obtained. The procedures and interpretations generally followed previous studies from this laboratory (17, 27-29).

The range of stability for the electrode in the absence of an added redox couple was determined from the CV behavior of p-Cu_2O in MeCN containing TBAP alone, as shown in Fig. 4(a). The dark current was very small up to $-$ 1.8V *vs.* SCE. Under illumination, no photocurrent was observed up to $-$ 1.5V. However, at more negative potentials a small and unstable photoinduced cathodic current was found, which probably involves reduction of the Cu_2O electrode perhaps involving trace impurities (*e.g.*, H_2O) in the solvent.

The addition of a reducible substance to the MeCN/TBAP solution generally did not produce an appreciable increase in the dark cathodic current for potentials up to $-$ 1.60V, demonstrating the expected absence of dark electron transfer to solution species at the p-type semiconductor/liquid interface. Under illumination, however, the photogenerated electrons at energies corresponding to the conduction bandedge can transfer to solution species, and significant photocathodic currents are produced. For example, the CV reduction of phthalonitrile [Ph(CN)$_2$] on Pt, given in Fig. 4(b), shows a reversible wave for the reduction to the radical anion at $-$ 1.72V *vs.* SCE. On p-Cu_2O, only a small dark reduction current is seen (Fig. 4c). However, under illumination, significant cathodic current flows with the onset at potentials more positive than those for reduction at Pt (Fig. 4d). Note, how-
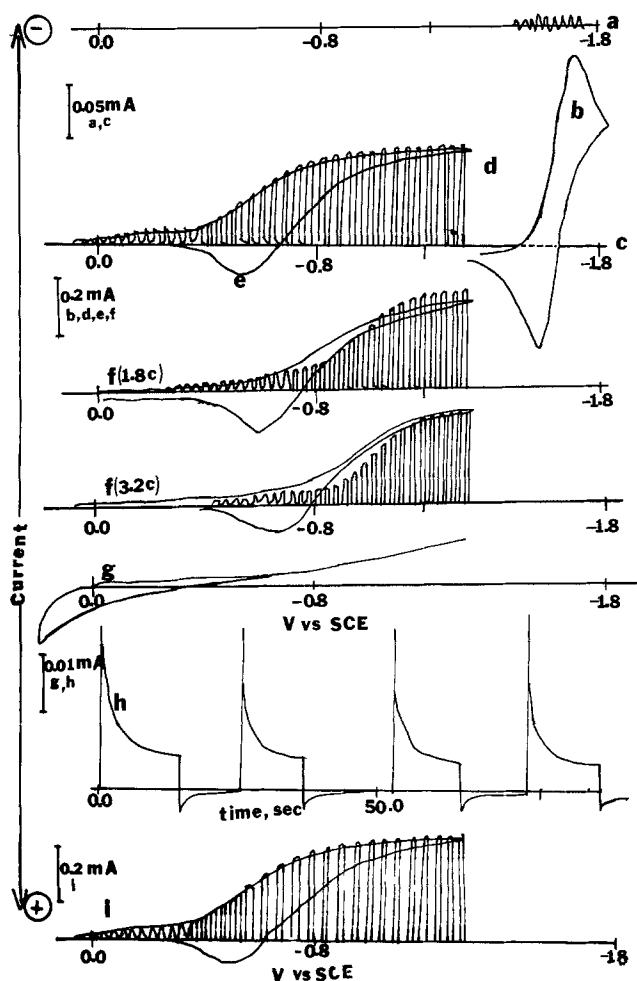
Fig. 4. Voltammetric curves of Pt and p-Cu_2O in MeCN containing 10 mM ($Ph(CN)_2$; 0.1M TBAP (supporting electrolyte). Light source, 450W xenon lamp. Scan rate = 50 mV/sec. (a) C-V curve on p-Cu_2O in dark and under illumination in MeCN containing 0.1M TBAP only; (b) cyclic voltammogram at Pt; (c) dark voltammetric curve on p-Cu_2O; (d) C-V characteristics under chopped light in p-Cu_2O before generating radical anions, in the dark; (e) C-V characteristic curve of p-Cu_2O under continuous illumination; (f) same as in (a-e) but after electrochemically generating anion radicals; (g) C-V curves on p-Cu_2O in dark after electrochemically generating anion radicals; (h) transient i-t curves of p-Cu_2O. The electrode was biased at −0.5V vs. SCE; (i) same as in (a-e) but after irradiation for 6 hr, p-Cu_2O electrode was biased at −0.3V vs. SCE.

ever, that although there is a considerable "underpotential" for the start of the reduction of $Ph(CN)_2$, the cathodic photocurrent rises rather slowly with potential and only attains a limiting value at $\sim$ −0.9V. This slow rise in cathodic photocurrent can be attributed to appreciable oxidation of the photogenerated reduced species, $Ph(CN)_2^{-}$, at potentials between the onset potential and the limiting one. This oxidation of the reduced form is apparent from the reverse scan (Fig. 4e), where the current crosses the zero current axis at more negative potentials than the original onset potential and the presence of photogenerated radical anion,

$Ph(CN)_2^{-}$ causes an anodic current flow. Similarly, if the initial scan is carried out with a solution that contains both parent and radical anion, the onset potential occurs at more negative values, $\sim$ −0.6V vs. SCE (Fig. 4f). Moreover, as the concentration of radical anion is increased, the onset potential also shifts toward more negative values. In Fig. 4g is shown the effect of radical anion on the behavior of p-Cu_2O in dark. The dark oxidation current begins at −0.6V. Thus the back-

oxidation of $Ph(CN)_2^{-}$ leads to the observed shape of the photocurrent-potential curve and the fact that the photocathodic current remains small up to −0.5V vs. SCE, even though the onset of photocurrent occurs near the flatband potential. The presence of surface recombination or back-reaction below −0.5V vs. SCE is also demonstrated by the transient photocurrent-time behavior of p-Cu_2O in MeCN containing TBAP, $Ph(CN)_2^{0/-1}$ (Fig. 4h). Upon illumination, the cathodic current shows a sharp increase, but then rapidly drops off as radical anion accumulates at the electrode surface. When the light is turned off, the current drops and an anodic current spike appears, representing oxidation of radical anion. At more negative potentials (e.g., −0.9V), only a flat photocathodic current transient appears, with no anodic dark transient. After continuous illumination for 6 hr, with the p-Cu_2O electrode held at −0.3V vs. SCE, the CV behavior was essentially unchanged (Fig. 4i), thus demonstrating the stability of the semiconductor electrode. The behavior of p-Cu_2O with $Ph(CN)_2$ was typical of that found with other redox couples. From the location of the energy levels of these couples with respect to the bandedges (Fig. 3), one would predict, based on the "'ideal" model of the semiconductor/liquid interface, that all of the couples would be photoreduced with the potential of the onset of photocurrent V_{on}, located near V_{FB}. This was found to be the case for solutions initially containing only the oxidized form of the couple. The values of V_{on} and V_{redox} are given in Table I. In all cases appreciable photocurrent flowed only at potentials significantly more negative than V_{on}. The limiting quantum efficiency for the photogeneration of

$Ph(CN)_2^{-}$, defined as the ratio of the current (in electrons/s-cm^2) to the absorbed light flux (in photons/s-cm^2), with the p-Cu_2O electrode held at a potential of − 1.0V where the limiting current is attained, was estimated at 500 nm. This value of λ corresponds to an energy greater than the bandgap of p-Cu_2O. The 500 nm radiation was obtained by interposing a Jarrel-Ash Company (U.S.A.) monochromator between the PEC cell and the xenon lamp (2500W operated at 1600W); the monochromatic light was focused on the p-Cu_2O electrode. The photocurrent, recorded on a Model 2000 X-Y recorder (Houston Instruments, Austin, Texas), was 0.70 $\mu A/cm^2$. The PEC cell was then replaced and the monochromatic light intensity, measured by a radiometer/photometer, Model 550-1 (Electro Optics Division) was 14.6 $\mu W/cm^2$. These values yield a monochromatic quantum efficiency of $\sim$ 10.5%.

Effect of pretreatment.—The nature of the electrode surface pretreatment, e.g., via etching, is known to affect the behavior and PEC performance of SC electrodes (30, 31). Four different etchants were used in this work, described in the experimental section. Electrodes treated with etchants (2), (3), or (4) gave large dark currents as compared to those with 1 (12M

Table I. Voltammetric data and onset potential of photocurrent

Electrode = p-Cu_2O, V_{FB} = +0.16V vs. SCE, N_A = 4.87 × 10^{16}/cm^3

Redox couple[a]	V_{redox} V vs. SCE	V_{on} V vs. SCE	V_{ph} = $\mid V_{redox} - V_{on} \mid$
$Ph(CN)_2^{(0/-1)}$	−1.72	+0.02	1.74
$Ph(NO_2)^{(0/-1)}$	−1.33	+0.03	1.36
$AB^{(0/-1)}$	−1.28	+0.04	1.32
$AQ^{(0/-1)}$	−0.96	+0.04	1.00
$BQ^{(0/-1)}$	−0.53	+0.06	0.59
$MV^{+2/+1}$	−0.43	0.00	0.43

[a] Abbreviations: $Ph(CN)_2$ = phthalonitrile; $Ph(NO_2)$ = nitrobenzene; AB = azobenzene; AQ = anthraquinone; BQ = benzoquinone; MV = methyl viologen.

HNO_3) (Fig. 5). Generally, electrodes that showed surfaces with large crystallites and grain boundaries, as produced by etching with 12M HNO_3, showed a better PEC performance than those with smooth and shiny surfaces [*e.g.*, as produced by etchant (4)].

Anodically grown Cu_2O *films.*—The PEC behavior of p-Cu_2O anodic films depended upon the electrochemical conditions employed for growing the oxide film and the pretreatment of the Cu electrode before film formation. The films produced in aqueous NaOH solutions by linearly scanning the potential showed better photoresponse than those prepared by galvanostatic oxidation. Among the Cu electrode pretreatments tried [etching with 6M HNO_3, etching with $FeCl_3$ in EtOH, electropolishing (20), or electropolishing with etching in $FeCl_3$], etching with HNO_3 produced electrodes which showed the largest photoeffects. Etching, with either $FeCl_3$ or the electropolished surfaces, yielded Cu_2O films which showed a poor photoeffect. For films grown by linear scans, the photoresponse depended upon the potential scan rate, v, for film growth. Films grown at very small v (0.02 mV/sec) exhibited better PEC behavior than those grown at higher scan rates (0.2 and 1.0 mV/sec). In the linear scan experiments, the formation of Cu_2O was characterized by a peak obtained at -0.4 to $-0.5V$ *vs.* SCE (20). To avoid conversion of the Cu_2O to CuO, the potential was not scanned beyond $-0.35V$ *vs.* SCE. Current-potential

curves in the dark and under chopped illumination for p-Cu_2O films (grown at 0.02 mV/sec in 1M and 5M NaOH) in MeCN/TBAP containing $Ph(CN)_2$ are given in Fig. 6. The photoresponse was clearly much greater for films grown in 5M NaOH. The beneficial effect of slow scan rate and higher NaOH concentration is probably caused by the formation of a less random and thicker film (20). Some improvement in the onset potential and photocurrent was achieved by etching the anodic Cu_2O film with 0.01M HNO_3 for 1-2 sec. Etching with a more concentrated HNO_3 solution (0.1M) destroyed the photoeffect, presumably because dissolution of the Cu_2O film occurred. Films grown in 10M NaOH gave a photoresponse similar to those grown in 5M NaOH at 0.02 mV/sec. Generally, however, the photocurrents at the anodic films were much smaller than those at the thermally grown material for similar solution and illumination conditions.

p-Cu_2O/MeCN PEC cells.—The CV behavior can be used as a guide for the construction of PEC photovoltaic cells, where the open-circuit potential of the semiconductor ideally (in the absence of recombination) approaches V_{FB} and the metal counterelectrode is at V_{redox}. Although the photocurrents found in the CV experiments with p-Cu_2O were rather small, the behavior of actual two-electrode photovoltaic cells is of interest because observed responses under these conditions insure that the effects seen are not merely caused by conductivity changes under illumination and allow an estimation of the actual power conversion efficiency of such devices. From the energy level diagram (Fig. 3) and the voltammetric measurements (Table I), cells containing $Ph(CN)_2$ would be expected to show the highest open-circuit voltage, V_{oc}, and the best performance. The following cell was constructed: p-Cu_2O/

MeCN, TBAP (0.1M), $Ph(CN)_2$ (10 mM), $Ph(CN)_2^-$ (0.1 mM)/Pt. The p-Cu_2O photocathode (0.14 cm²) and the Pt gauze (40 cm²) counterelectrode were spaced about 1.0 cm, with the p-Cu_2O electrode about <0.1 cm from the cell window. The *i*-*V* characteristic of such a cell, obtained with different load resistances, is shown in Fig. 7. The open-circuit photovoltage was 0.3V, the short-circuit photocurrent density was 0.4 mA/cm², and the fill factor was 0.51. Note that this open-circuit voltage is considerably lower than the value predicted from voltammetric measurements conducted with solutions in the absence of appreciable

$Ph(CN)_2^-$. It is, however, about the same as that found with solid-state p-Cu_2O cells (12). From the
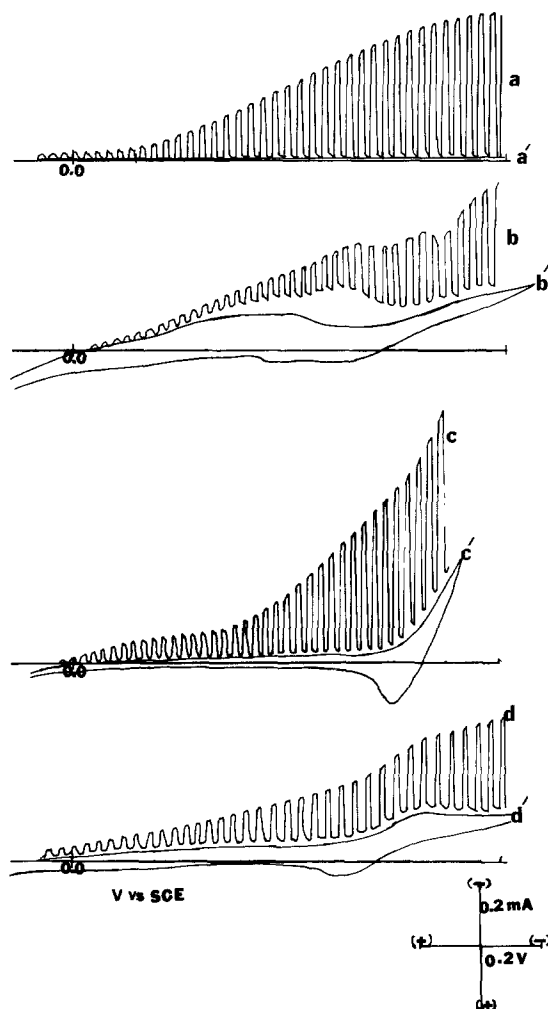

Fig. 5. Current-potential characteristics under chopped light on p-Cu_2O in MeCN containing 0.2M $PhNO_2$, 0.1M TBAP (supporting electrolyte). Light source, 450W xenon lamp. Scan rate, 50 mV/sec. (a) p-Cu_2O treated with 12M HNO_3; (b) p-Cu_2O treated with 6M HNO_3; (c) p-Cu_2O treated with H_2SO_4: H_2O_2:H_2O = 3:1:1; (d) p-Cu_2O treated with NHO_3:H_3PO_4; acetic acid = 17:41.5:4.15. a′, b′, c′, and d′ are in the dark.
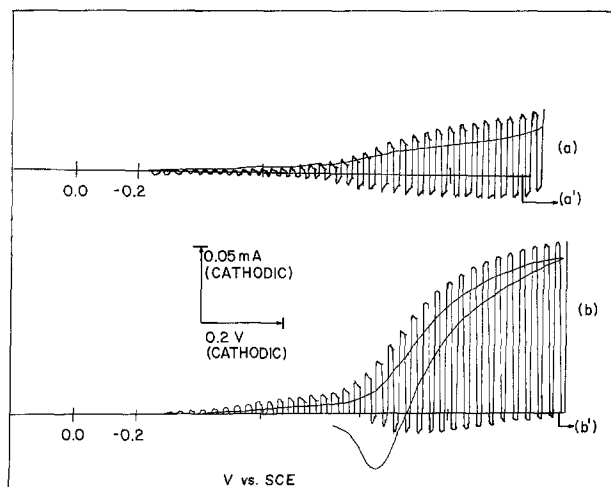

Fig. 6. Current-potential characteristics under chopped light on p-Cu_2O (anodically oxidized) in MeCN containing 10 mM $PhCN_2$; 0.1M TBAP. Light source, 450W xenon lamp. Scan rate, 50 mV/sec. (a) p-Cu_2O prepared in 1M NaOH; (b) p-Cu_2O prepared in 5M NaOH. a′ and b′ are in the dark.
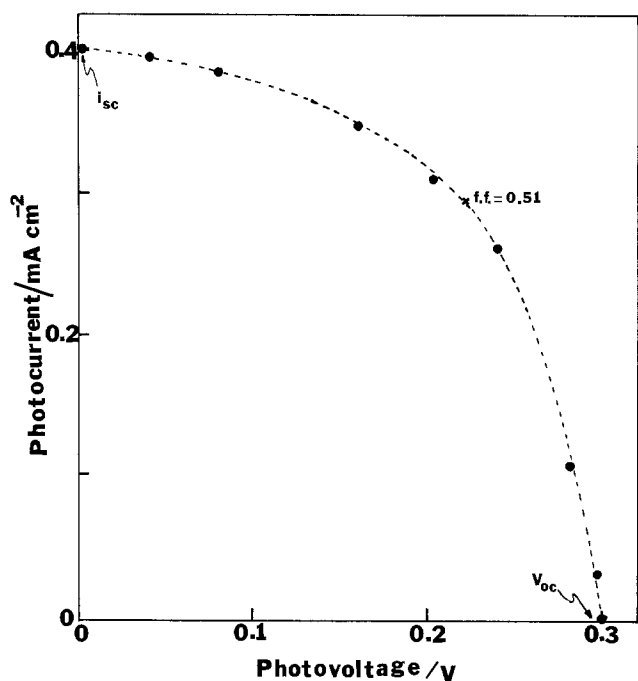
Fig. 7. Photocurrent-photovoltage characteristic of the cell p-Cu$_2$O/MeCN, 10 mM Ph(CN)$_2$; 0.1 mM Ph(CN)$_2$⁻ TBAP, 0.1 M/Pt various load resistances. Irradiation source, 450W xenon lamp.

data in Fig. 7 and the light flux of 120 mW/cm^2, the overall optical-to-electrical energy conversion efficiency, uncorrected for absorption and reflectivity losses, was calculated to be ~0.05%. This low value can probably be attributed to rapid recombination processes both within the bulk p-Cu$_2$O and at the interface. The currents were not limited by mass transfer and were unaffected by stirring. The Ph(CN)$_2$⁻ was intentionally kept at a low concentration to decrease the light adsorption by this intensely colored species and to minimize the back-reaction at the p-Cu$_2$O surface. The photocurrent as a function of time is shown in Fig. 8. The photocurrent was fairly stable for at least 6 hr at which time the experiment was terminated.

Scanning electron micrographs of different thermally grown specimens after etching or polishing are given in Fig. 9. Samples etched with HNO$_3$ (Fig. 9a) showed
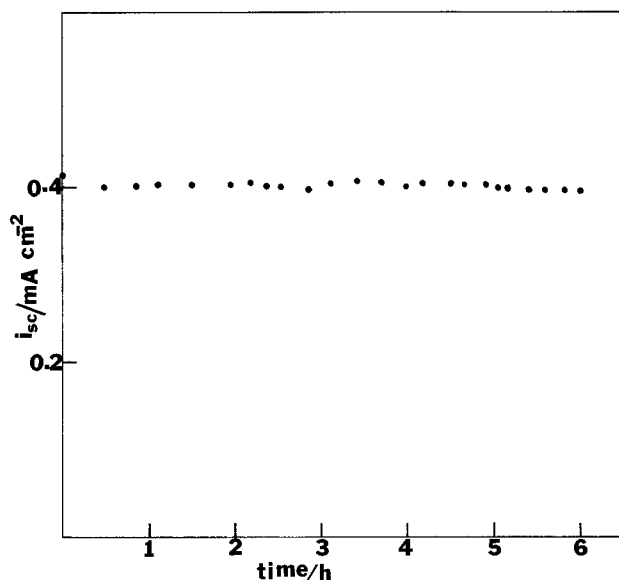

Fig. 8. Plot of photocurrent-output density of the cell p-Cu$_2$O/MeCN, 10 mM Ph(CN)$_2$, 0.1 mM Ph(CN)$_2$⁻; TBAP = 0.1 M/Pt as a function of time. Light source, 450W xenon lamp.

well-developed crystallites with distinct boundaries. While some of the crystallites were rather large, zones of smaller crystallites were also found. There was no marked change in the morphology of p-Cu$_2$O surfaces after the PEC measurements (Fig. 9b). The surfaces of electrodes either polished with Al$_2$O$_3$ (0.5 μm) or etched with HNO$_3$: acetic acid: H$_3$PO$_4$ were smooth (Fig. 9c, d). To test if the small crystallites and numerous grain boundaries found with the 12M HNO$_3$ etched samples were responsible for the low photovoltages and efficiencies, an electrode was prepared in which all of the small crystallites were covered with silicone rubber sealant, leaving only a single large crystal exposed to the solution. However, PEC measurements with this electrode showed no apparent increase in either the photovoltage or photocurrent density. This suggests that there may be inherent problems in the efficiency of p-Cu$_2$O itself, and that marked improvement in the efficiency with this material may be difficult.

Conclusions

The p-Cu$_2$O photocathode is stable in MeCN containing a number of different redox couples under irradiation. The photopotential, V_{ph}, equal to $(V_{redox} - V_{on})$, increases linearly with V_{redox}, with a slope near one. The onset of photocurrent is located, for all couples investigated, near the flatband. Pretreatment of the electrode plays an important role on the PEC performance of p-Cu$_2$O, and etching with 12M HNO$_3$ was found to give a reasonable photocurrent and small dark cathodic current. The 12M HNO$_3$ etched surface, which looks matte and polycrystalline with distinct grain boundaries, exhibited better PEC behavior than the one which was shiny and smooth (e.g., produced by an HNO$_3$: acetic acid: H$_3$PO$_4$ etching).

The overall conversion efficiency of optical-to-electrical energy for the PEC photovoltaic cells was low, < 0.1%. A brief comparison of the liquid junction photovoltaic cells with the solid-state cells is in order. Under similar irradiation intensities, the Schottky barrier Cu/p-Cu$_2$O cells under the best conditions are reported to show an efficiency of 0.8% (12). The observed open-circuit photovoltage (0.30V) and fill factor (0.39) are comparable to the values in the liquid junction cells, so that the lower efficiency can be traced to lower short-circuit photocurrents. Indeed, even in the solid-state cells, encapsulation of the cell with epoxy is required for optimum performance. This encapsulation not only reduced reflection losses but also decreased the observed dark current. Moreover, the resistivity of our p-Cu$_2$O was ~ 3-4 times that of the Cu$_2$O used in the solid-state cells and, in the absence of more promising efficiencies, we did not find it worthwhile to attempt to optimize the semiconductor material. In general, the low photocurrents and efficiencies in the liquid junction cells probably can be attributed to rapid surface and bulk recombination of the photogenerated charge carriers. On the basis of these results and the fact that efficiencies > 1% have not been reported for solid-state cells, unless a significant improvement in the materials, characteristics, and efficiency can be obtained, p-Cu$_2$O does not seem to be a promising candidate for PEC solar energy conversion devices.

Acknowledgment

Fig. 9. Scanning electron micrographs of p-Cu_2O, thermally grown samples differently etched: (a) Etched with 12M HNO_3, before PEC measurement. (b) Etched with 12M HNO_3, after PEC measurement. (c) Al_2O_3 (0.5 μm) polished. (d) Etched with HNO_3:H_3PO_4:acetic acid = 17:4.15:41.5 by volume.
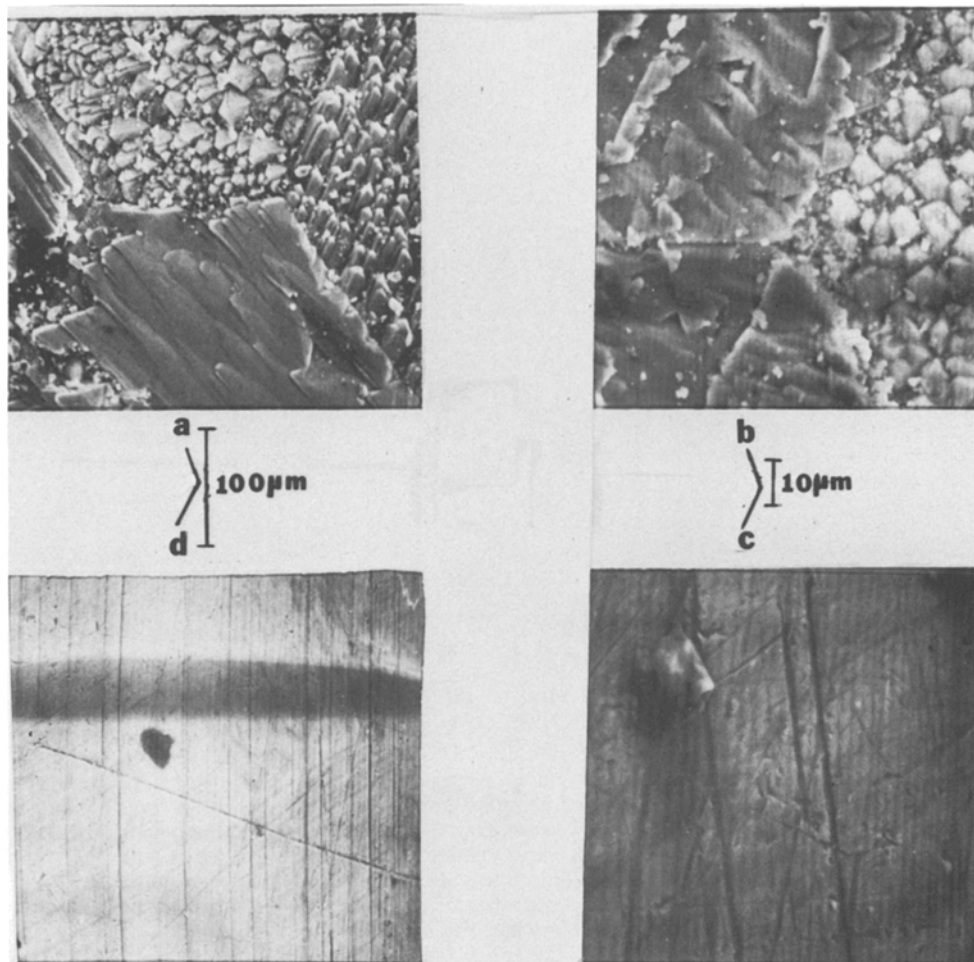
Manuscript submitted Dec. 22, 1980; revised manuscript received April 9, 1981.

Any discussion of this paper will appear in a Discussion Section to be published in the June 1982 JOURNAL. All discussions for the June 1982 Discussion Section should be submitted by Feb. 1, 1982.

REFERENCES

1. B. J. Wood, H. Wise, and R. S. Yolles, *J. Catal.*, **15**, 355 (1969).
2. L. L. Holbrook and H. Wise, *ibid.*, **27**, 322 (1972).
3. M. O'Keeffe and F. S. Stone, *Proc. R. Soc. London, Ser. A*, **267**, 501 (1962).
4. S. R. Morrison, *J. Catal.*, **34**, 462 (1974).
5. G. F. J. Garlick, "Photoconductivity," Handbuch der Physik XIX, pp. 377-380, Springer, Berlin, West Germany (1956).
6. J. A. Assimos and D. Trivich, *Phys. Status Solidi A*, **26**, 477 (1974).
7. G. P. Pollack and D. Trivich, *J. Appl. Phys.*, **46**, 163 (1975).
8. J. Bloem, *Philips Res. Rep.*, **13**, 167 (1958).
9. R. S. Toth, R. Kilkson, and D. Trivich, *Phys. Rev.*, **122**, 482 (1961).
10. M. O'Keeffe and W. J. Moore, *J. Chem. Phys.*, **35**, 1324 (1961).
11. M. H. Zirin and D. Trivich, *ibid.*, **39**, 870 (1963).
12. D. Trivich, E. Y. Wang, R. J. Komp, and F. Ho, *Conf. Rec. IEEE Photovoltaic Spec. Conf.*, **12**, 875 (1976).
13. K. Hauffe and K. Reinhold, *Ber. Bunsenges. Phys. Chem.*, **76**, 616 (1972).
14. U. Bertocci and D. R. Turner, in "Encyclopedia of the Electrochemistry of the Elements," Vol. 2, A. J. Bard, Editor, pp. 457-463 and numerous references therein, Marcel Dekker, New York (1974).
15. K. Hardee and A. J. Bard, *This Journal*, **124**, 215 (1977).
16. J. S. Anderson and N. N. Greenwood, *Proc. R. Soc. London, Ser. A*, **215**, 353 (1952).
17. G. Nagasubramanian and A. J. Bard, *This Journal*, **128**, 1055 (1981).
18. R. S. Toth, R. Kilkson, and D. Trivich, *J. Appl. Phys.*, **31**, 1117 (1960).
19. S. L. Marchiano, C. I. Elsner, and A. J. Arvia, *J. Appl. Electrochem.*, **10**, 365 (1980).
20. V. Ashworth and D. Fairhurst, *This Journal*, **124**, 506 (1977).
21. V. A. Myamlin and Y. V. Pleskov, "Electrochemistry of Semiconductors," Plenum Press, New York (1967).
22. H. Gerischer, in "Advances in Electrochemistry and Electrochemical Engineering," Vol. 1, P. Delahay and C. W. Tobias, Editors, pp. 139-232, Interscience, New York (1961).
23. R. Memming, in "Electroanalytical Chemistry," Vol. 11, A. J. Bard, Editor, pp. 1-84, Marcel Dekker, New York (1979).
24. K. Kojendahl, *Z. Phys. Chem.*, **B20**, 54 (1933).
25. A. G. Zhilic, J. Halpern, and B. P. Zakharchenya, *Phys. Rev.*, **188**, 1294 (1969).
26. V. A. Fishman and A. J. Bard, *Anal. Chem.*, **52**, 1723 (1980), and references therein.
27. P. A. Kohl and A. J. Bard, *This Journal*, **126**, 59 (1979).
28. P. A. Kohl and A. J. Bard, *J. Am. Chem. Soc.*, **99**, 7531 (1977).
29. P. A. Kohl and A. J. Bard, *This Journal*, **126**, 603 (1979).
30. B. A. Parkinson, A. Heller, and B. Miller, *ibid.*, **126**, 954 (1979).
31. R. L. Van Meirhaeghe, F. Cardon, and W. P. Gomes, *Ber. Bunsenges. Phys. Chem.*, **83**, 236 (1979).